COBEM 2023 27TH INTERNATIONAL CONGRESS OF MECHANICAL ENGENEERING

ABCM Brazilian Society of Mechanical Sciences and Engineering
27th ABCM International Congress of Mechanical Engineering
December 04-08, 2023, Florianópolis-SC, Brazil

COB-2023-2053
NONLINEAR SIMULATION OF TRANSMISSION GEARS COUPLING CONSIDERING THE IMPACT PAIR EFFECT

Nícolas Londero Gass
Alberto Luiz Serpa
Universidade Estadual de Campinas, Cidade Universitária Zeferino Vaz, Campinas - SP
n203980@dac.unicamp.br, alserpa@unicamp.br

Abstract. *This paper presents a methodology for evaluating the dynamic behavior of a geared transmission system. The objective is to identify the sources of impulsive impacts that generate the clunk noise phenomenon and evaluate their effect on the torsional vibration of the system by using the "impact pair" model to describe its behavior. The "impact pair" response is obtained using the Newmark nonlinear method, which simulates the system's nonlinear behavior, considering the effect of clearances in the model. The validation process compares the results obtained with Newmark nonlinear method and Simcenter AMESim software. Previous studies have emphasized the importance of analyzing the effects of transmission system parameters on its dynamic behavior, the loading force on the transmission system can affect the nonlinearity behavior, and evaluating the minimum loading torque required to cause the clunking noise is also crucial. In conclusion, the paper proposal involves representing the torsional vibration analysis of transmission systems, using the "impact pair" model, and considering the effect of nonlinearity in the system. The results obtained can be used to improve the safety, efficiency, and reliability of transmission systems, thus reducing the risk of failures.*

Keywords: *Impact pair model, Clunk noise, Transmission nonlinearity, Dynamic response.*

1. INTRODUCTION

The investigation of transmission noise and vibration has garnered significant attention due to the growing demand for improved product design and higher quality standards. Among the various vibroacoustic phenomena in these systems, two noteworthy examples are gear rattle and clunk noise. This article provides a comprehensive overview of evaluating these events through a simplified and precise methodology, utilizing lumped parameters and Newmark's integration method. Furthermore, it compares their outcomes with Simcenter AMESim results to verify its accuracy.

Clunk noise is characterized by low to mid-frequency noise that arises during driving situations when the transmission system experiences torque inversions, referred to as tip in / tip out, where the inertia torque exceeds the load torque (Comparin (1988)). This results in gear separation and impacts (Crowther *et al.* (2005)). Clunk noise can be induced by gear shifting while driving and abrupt clutch pedal release. In geared systems, torque inversions cause the system to traverse its clearances (Crowther *et al.* (2005)), which are essential for proper operation but contribute to nonlinear behavior. Consequently, impulsive impacts occur between gear pairs, leading to the perceptible clunk noise and gear rattle experienced by vehicle users.

Gear rattle, another vibroacoustic phenomenon in transmission systems, involves the rapid oscillation of gears when subjected to transient excitation or sudden load changes (Comparin (1988)). It manifests as a high-frequency noise and can be influenced by gear backlash and transmission error.

Recent studies have identified several key project parameters that influence vibroacoustic behavior, including loading torque (Gurm *et al.* (2007)), varying mesh stiffness, gear mesh damping, gear pressure angle, helix angle, and clearance magnitude (Chen *et al.* (2018)). The lumped parameters method can be employed to analyze the impact of these parameters on vibroacoustic behavior, with a specific focus on the primary vibration source component: the gear pairs within the transmission system.

The impact pair methodology, introduced by Comparin (Comparin (1988)), offers a practical approach to simplifying gear pairs in a lumped parameters analysis. In conjunction with this methodology, selecting a suitable time integrator plays a crucial role in accurately handling the system's nonlinearities resulting from changes in stiffness. One integrator capable of evaluating phenomena associated with clunk noise is Newmark's nonlinear time integrator (Chopra (1995)), which will be briefly explained in the subsequent section.

2. NONLINEAR NEWMARK METHOD

The Newmark method was developed in 1959 by N. M. Newmark as a time-domain integrator for second-order differential equations (Geradin and Rixen (2014)). It deals with formulating dynamic equilibrium, considering the nonlinearity

present in the system, such as impulsive impacts. The method is applied to solve systems represented in the following form for particular linear cases (Geradin and Rixen (2014)):

$$\begin{aligned} &P(\dot{u}, u) = C\dot{u} + Ku \\ &M\ddot{u} + P(\dot{u}, u) = F(t) \\ &u_0, \dot{u}_0 \text{ given} \end{aligned} \tag{1}$$

where M, C, K, and F are the mass, damping, stiffness matrices, and force vector, which are known parameters of the system, and $\ddot{u}, \dot{u}$ and u are the acceleration, velocity, and displacement of the system. This method considers the relationships between internal and external, dissipative, and restoring forces. The nonlinear behavior is incorporated through time iteration to obtain the correct structural response.

To configure the nonlinear Newmark integration method, some initial variables of the algorithm must be defined. These variables include the time discretization to be used (Δt), the initial acceleration $\ddot{u}_0$, the tangent stiffness matrix K_t, and the auxiliary variables $a_{1,2,3,4}$. The calculation of the initial acceleration requires an estimation of the internal efforts of the system, which are related to the elastic and dissipative forces of the system (Chopra (1995)).

The tangent matrix is essential for calculating the correction of the solutions during the iterative process. Using as an example a cubic spring, the formulation of the internal efforts of a nonlinear system and the calculation of the acceleration at any given time n is given by:

$$\begin{aligned} &P_n = C\dot{u}_n + Ku_n + \alpha u_n^3 \\ &\ddot{u}_n = M^{-1}(F_n - P_n) \end{aligned} \tag{2}$$

where γ and β are parameters associated with the quadrature scheme, which plays an essential role in the stability and accuracy of the solution (Geradin and Rixen (2014)) and can be used in the following configurations: Linear acceleration interpolation with $\gamma = \frac{1}{2}$, $\beta = \frac{1}{6}$; and Average acceleration with $\gamma = \frac{1}{2}$, $\beta = \frac{1}{4}$. For the application of this paper, the linear acceleration was chosen. Thus, the value of the internal forces P_0 is estimated. With these variables, the value of the initial acceleration $\ddot{u}_0$ is estimated (Chopra (1995)). The terms related to damping and stiffness correspond to the linear response of the system, while αu_{n+1}^3 is related to the nonlinear behavior of the system, where α is the nonlinearity factor that determines the intensity of the nonlinear effect on the system response.

After incorporating the influence of the cubic spring in the system, the next step is to calculate the iterative solutions for each integration point in the time domain, including the displacements, velocities, and accelerations for the next time step, represented by $n+1$. The equations for calculating the estimated displacements, velocities, and accelerations at time $n+1$ are:

$$\begin{aligned} &\ddot{u}_{n+1}^* = 0 \\ &\dot{u}_{n+1}^* = \dot{u}_n + a_1\ddot{u}_n \\ &u_{n+1}^* = u_n + \Delta t\, \dot{u}_n + a_2\ddot{u}_n \end{aligned} \tag{3}$$

The calculation of the residual is performed at each iteration to assess the convergence of the results and perform a correction for the next step. To guarantee that the solution converges, the iterative Newton-Raphson (NR) method is used, which is based on estimating the residual Ψ_{n+1}, which is given by:

$$\Psi_{n+1} = M\ddot{u}_{n+1} + P(\dot{u}_{n+1}, u_{n+1}) - F_{n+1} \tag{4}$$

In cases where the convergence is not satisfied, the solution correction process is continued. The displacement increment Δu is required to make the corrections and is computed according to the NR as:

$$S\Delta u = -\Psi_{n+1} \tag{5}$$

where Δu is the displacement increment, Ψ_{n+1} is the previously obtained residual, and the tangent matrix and tangent stiffness are given by:

$$\begin{aligned} &K_t = \frac{\partial P}{\partial u} \\ &S = Ma_4 + Ca_3 + K_t \end{aligned} \tag{6}$$

After obtaining Δu, the corrections are applied to the acceleration, velocity, and displacement results (Geradin and Rixen (2014)), according to:

$$\begin{aligned} \ddot{u}_{n+1} &= \ddot{u}^*_{n+1} + a_4 \Delta u \\ \dot{u}_{n+1} &= \dot{u}^*_{n+1} + a_3 \Delta u \\ u_{n+1} &= u^*_{n+1} + \Delta u \end{aligned} \tag{7}$$

3. NONLINEAR MODEL PARAMETERS

A simple representation of the initial nonlinear model is depicted in Fig. 1, including the system's stiffness nonlinear factor represented by $K + \alpha$.

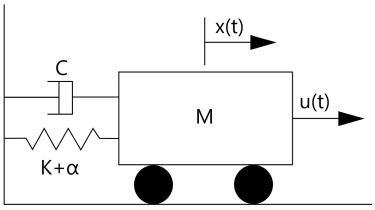

Figure 1. Example of mass-spring-damper model.

Different applied forces $u(t)$ were considered, such as constant force (Force 1), harmonic force (Force 2), and step force with finite duration (Force 3). The corresponding graphs for amplitude by the time of these applied forces are shown in Fig. 2.

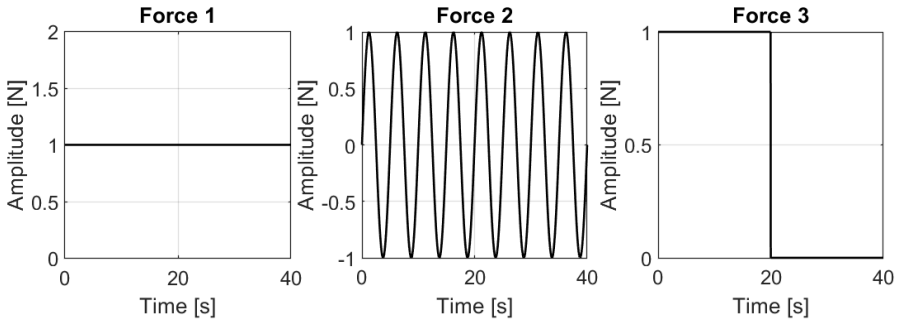

Figure 2. Applied forces in time used in the model.

A commercial tool, AMESim software, was employed to verify the results obtained from the nonlinear Newmark method. Initially, the responses for the forces used in the Newmark model, implemented in MATLAB, were assessed.

To determine if the results were accurate, a sensitivity analysis was conducted by changing the value of Δt between 0.1, 0.01, 0.001, and 0.0001, and a total time of 40 seconds to assess the convergence of the results. The convergence analysis results revealed that the nonlinear Newmark method, MATLAB Lsim function, and AMESim results were similar.

3.1 NEWMARK AND AMESIM RESULTS

The nonlinear Newmark method implemented in MATLAB was tested by varying the nonlinear constant (α) and the magnitude of the applied force (F_{mag}). The value of α directly affects the system's spring stiffness, where negative values decrease stiffness and positive values increase stiffness, depending on the force magnitude.

To ensure non-negative spring stiffness, three values of α were chosen for comparison: $\alpha = 0.1$, $\alpha = 0$, and $\alpha = -0.1$. These values represent three distinct system behaviors: increasing stiffness with $\alpha = 0.1$, decreasing stiffness with $\alpha = -0.1$, and linear behavior with $\alpha = 0$ (considering $K_s = Kx + \alpha x^3$ as an example). To confirm the accuracy of the MATLAB results, we replicated the model in AMESim, as depicted in Figure 3.

The configuration shown in Fig. 3 consists of components arranged from left to right: an input signal in red, representing the applied force, a signal transducer to force (in green), a lumped mass block, a displacement acquisition probe, which is connected to an equation block based on displacement, and connected to a variable stiffness spring and damper element, and a rigid support at the end of the far right end.

The equation block based on displacement is where the nonlinearity effect is included. Using a nonlinear cubic spring as an example, as mentioned before, the equation to be entered in the equation block should be $f(x) = Kx + \alpha x^3 = K_s$. Kx represents the linear term, and αx^3 represents the nonlinearity related to the cubic spring.

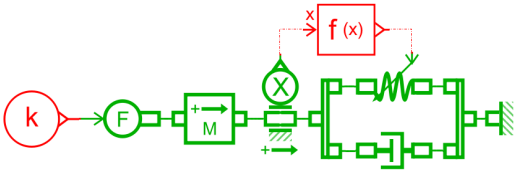

Figure 3. AMESim nonlinear model.

The model was tested using the same α values as mentioned before but with a higher force magnitude for all forces proposed to observe the dynamic response with nonlinearities. The results of these variations for force 1 can be observed in Fig. 4, and for forces 2 and 3 in Fig. 5.

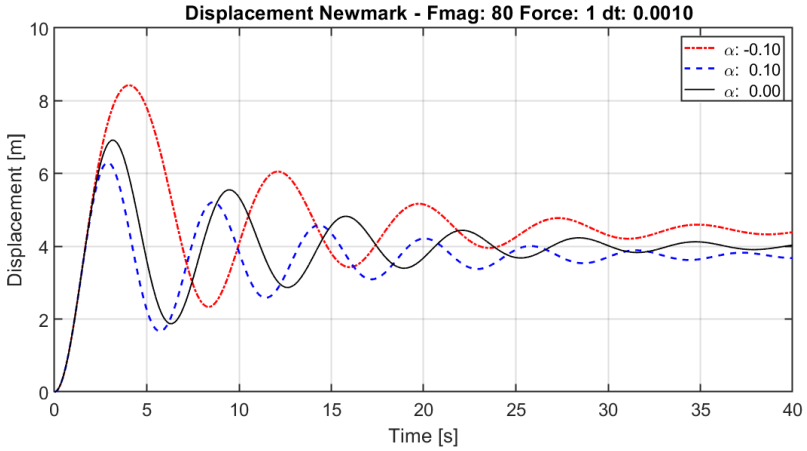

Figure 4. Newmark's displacement results for the linear model (black), nonlinear positive (blue), and nonlinear negative (red).

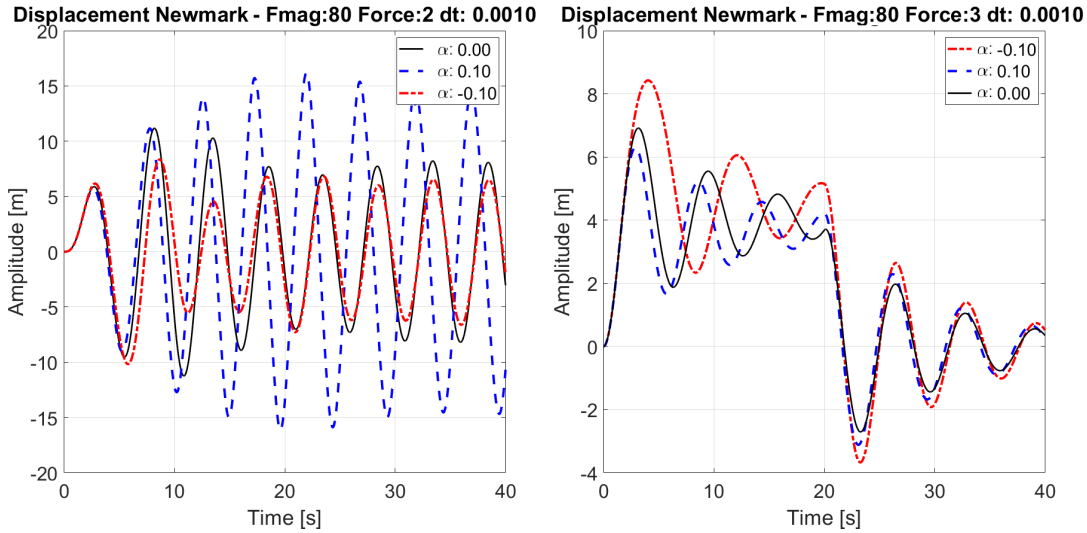

Figure 5. Newmark's displacement results for the linear model (black), nonlinear positive (blue), and nonlinear negative (red).

Figure 4 highlights a significant difference between the results for each established value of α. It shows the variation in displacement amplitude for the three values of the nonlinear constant. For $\alpha = 0.1$, the block displacement amplitude decreases due to increased system stiffness caused by positive nonlinearity. Additionally, noticeable phase shifts in the evaluated displacements are observed when $\alpha = 0.1$ (blue line), resulting in a shorter oscillation period than the linear model ($\alpha = 0$) and negative nonlinearity. These phase shifts occur due to increased system stiffness, leading to an increased resonance frequency and a shorter oscillation period.

Figure 5 right shows a similar behavior from the previous result, related to amplitude and phase shifts. The left figure depicts a different behavior since the negative nonlinearity displays a smaller amplitude than the linear or positive

nonlinearity response. In all evaluated cases, the results between AMESim and Newmark demonstrated convergence. Figure 6 compares the results for the constant applied force of 80 N using $\Delta t = 0.001$, displaying both positive and negative nonlinearity factor results.

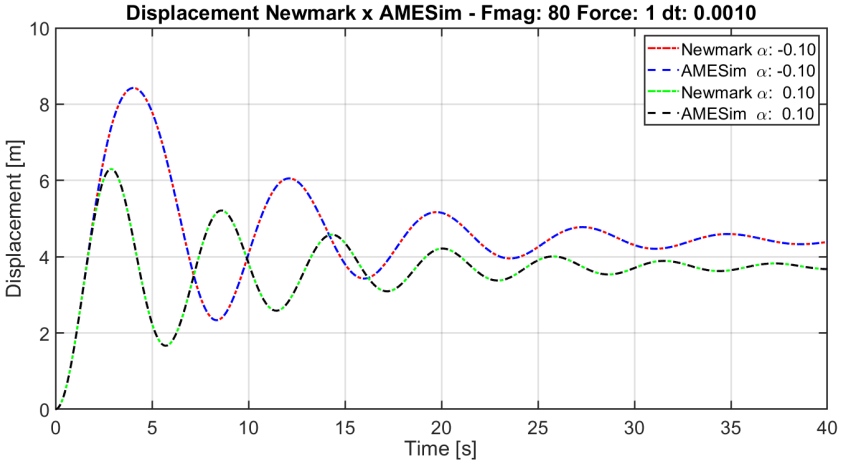

Figure 6. Comparison between Newmark's and AMESim displacements, including positive and negative nonlinearity.

Figure 6 focuses explicitly on the results considering the force with a magnitude of 80 N, as this configuration revealed the most significant differences in the system's behavior for each chosen nonlinear factor. The red and blue lines represent the Newmark method and AMESim results using a nonlinear factor of $\alpha = -0.1$. The green and black lines represent the Newmark method and AMESim results using a nonlinear factor of $\alpha = 0.1$. The graph analysis demonstrates the convergence of results, showing similar behavior for both methods.

The differences between displacement results were analyzed using the mean absolute error (MAE) and the mean percentage error (MPE). For each applied force (1 to 3), errors were calculated for positive and negative nonlinear factors (α). Table 1 presents the differences obtained between the integration methods.

Table 1. Mean Absolute Error (MAE) and Mean Percentual Error (MPE) differences between AMESim-Newmark displacements.

	Nonlinear factor α	**AMESim-Newmark (MAE)**	**AMESim-Newmark (MPE%)**
Force 1	0.1	6.79E-07	1.59E-05
	-0.1	4.20E-07	1.28E-05
Force 2	0.1	7.20E-07	1.87E-03
	-0.1	6.01E-06	2.46E-03
Force 3	0.1	6.08E-04	3.52E-01
	-0.1	5.15E-04	2.78E-01

The results presented in Table 1 demonstrate a good displacement convergence in the evaluated cases, regardless of the nonlinear factor used. In case 3, an increase in the results difference is observed, which can be attributed to the discrepancy after the value changes in the applied force vector. The obtained mean percentage error values support this fact.

The variable stiffness results obtained using Newmark and AMESim were compared for a deeper investigation of the model behavior. The comparison between the results is illustrated in Fig. 7.

The graph presents the system's results using $\alpha = 0.1$, obtained by Newmark (dashed green) and AMESim (dashed black), exhibiting identical behavior over time. The results using $\alpha = -0.1$ are also displayed, with Newmark shown in dashed red and AMESim in dashed blue, demonstrating good coherence. With the nonlinearity factor $\alpha = 0.1$, an increase in spring stiffness (hardening) is observed, while with $\alpha = -0.1$, a decrease in stiffness (softening) occurs.

To evaluate the behavior and stability of the system, phase diagrams of the model were plotted using three configurations of the nonlinearity factor, with the same force and force amplitude applied. The force magnitude was chosen to generate nonlinear dynamic responses by the system, using $Fmag = 80$. Figure 8 shows the results for the model, illustrating the influence of nonlinearity on its behavior.

Figure 8 reveals that the negative nonlinearity factor (in red) results in a more significant displacement along the horizontal axis due to the "softening" phenomenon. On the other hand, the positive nonlinearity factor (in blue) leads to a smaller displacement due to the "hardening" effect.

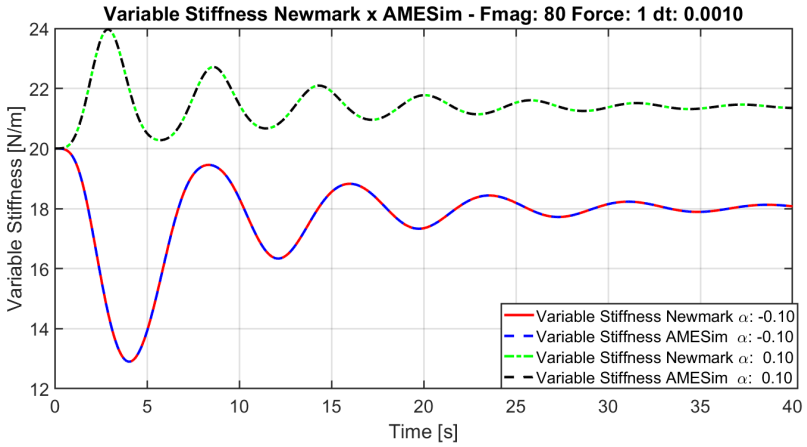

Figure 7. Comparison between Newmark's and AMESim variable stiffness for positive and negative nonlinearity.

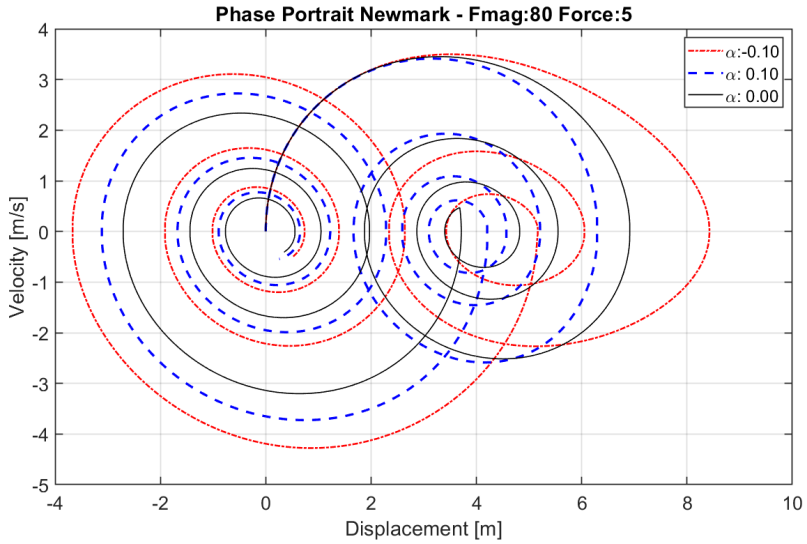

Figure 8. Phase portrait results of the model, using three nonlinear factors for the finite duration step force.

In comparing the results obtained from AMESim and Newmark, phase diagrams were plotted separately for each value of the nonlinearity factor, allowing for better visualization of the differences. The complete graph can be seen in Fig. 9.

In the left graph of Fig. 9, the results using $\alpha = -0.1$ are presented in the center $\alpha = 0$, and in the right $\alpha = 0.1$. Dotted red lines represent the results from Newmark, while dashed blue lines represent the results from AMESim. It can be observed that the results between the two software tools are identical for all values of α used.

4. IMPACT PAIR

An important consideration is the simplification of the system into impact pairs (IP), considering the contact between the gears as damping (D_M) and stiffness (K_M) that varies according to the gear contact. The system is simplified in lumped parameters, where the gears are considered inertia components and shafts as torsional spring elements (Comparin (1988)).

Figure 10 illustrates the methodology of the IP, as employed by Comparin (Comparin (1988)), where θ_{GI} and θ_{GO} represent the angular displacements of the input torque gear and output torque gear, respectively; R_{GI} and R_{GO} denote the base radius of the gears; I_{GI} and I_{GO} represent the moments of inertia of the gears; K_{B1} and K_{B2} represent the shaft stiffness; θ_{B1} and θ_{B2} denote the angular displacements at the end of each side of the shaft; and T_{GL} represents the loading torque of the output gear.

The equations of motion, which describe the torsional behavior of IP shown in Fig. 10, are given by:

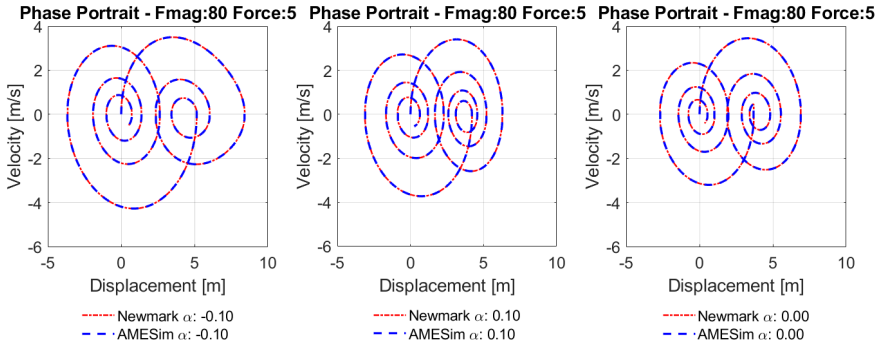

Figure 9. Phase portrait comparison AMESim-Newmark, using three nonlinear factors for the finite duration step force.

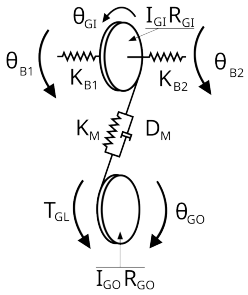

Figure 10. Impact pair model.

$$
\begin{aligned}
&I_{GI}\ddot{\theta}_{GI} + K_{B1}(\theta_{GI} - \theta_{B1}) + K_{B2}(\theta_{GI} - \theta_{B2}) + K_M R_{GI} f_g(\delta) + D_M R_{GI}\dot{\theta}_{GI} = 0 \\
&I_{GO}\ddot{\theta}_{GO} - K_M R_{GO} f_g(\delta) - D_M R_{GO}\dot{\theta}_{GO} = -T_{GL} \\
&\delta_g = \theta_{GI} R_{GI} - \theta_{GO} R_{GO}
\end{aligned} \tag{8}
$$

where δ_g is the relative displacement between the gears, $f_g(\delta)$ is the nonlinear force, which will introduce the nonlinearity in the model, given from the varying gear mesh stiffness. The nonlinear force can be written as:

$$
f(\delta) = \begin{cases} \delta - b + \alpha b & \delta > b \\ \alpha\delta & -b < \delta < b \\ \delta + b - \alpha b & -b > \delta \end{cases} \tag{9}
$$

where α is the nonlinear factor, which will dictate the intensity of the nonlinearity. The nonlinearity is considered weak when α has a value close to 1, and when α is significantly greater or smaller than 1, nonlinearity is considered substantial (Comparin (1988)). This effect is represented in the example in Fig. 11, where the nonlinear forces are represented from left to right using $\alpha = 0$, $\alpha = 0.3$, and $\alpha = 0.6$.

Figure 11 shows that as the value of α gets closer to 1, the nonlinearity presents almost a linear behavior.

4.1 IMPACT PAIR RESULTS COMPARISON

The same Impact Pair model was implemented in AMESim and Newmark method to assess and compare its behavior. The model was tested using a applied force similar to force 1, used in the 1 DOF model (shown earlier), but in this case representing an applied torque. The signal generated is received by a signal to a rotation speed converter, followed by an angular displacement probe. To account for inertia, an inertia component was introduced before the input gear, symbolizing the input gear's inertia. In contrast, the inertia for the output gear is situated within the gear component itself. The output gear is linked to a rotary spring, which, in turn, is connected to a zero angular speed source. This configuration is designed to introduce torsional resistance into the model. Figure 12 shows the model sketch used in AMESim.

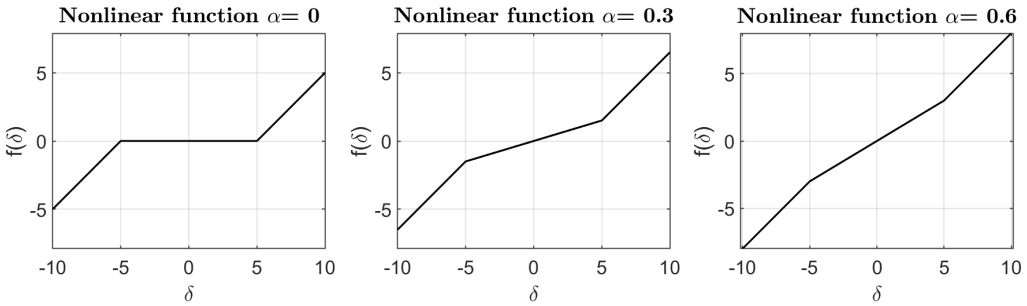

Figure 11. Nonlinear forces, using $\alpha = 0, \alpha = 0.3$, and $\alpha = 0.6$.

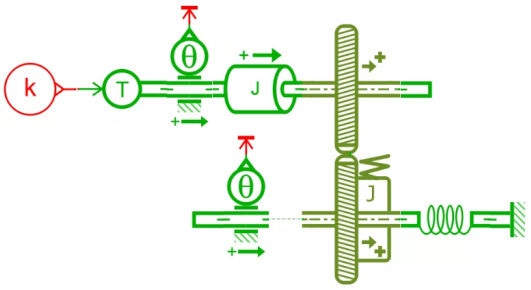

Figure 12. Impact pair model built in AMESim.

The model's results were observed with two values of backlash between gears: $0mm$ and $1mm$, over a duration of 5 seconds. The analysis involved varying the time step Δt between 0.01, 0.001, and 0.0001, revealing a strong similarity between the Newmark and AMESim results.

The results observed were the angular displacement, angular velocity, angular acceleration and backlash and contact condition for each gear within the model. Figure 13 displays the results for the model with no backlash, with Newmark method results represented by solid lines labeled 'NM' and AMESim results depicted with dashed lines labeled 'AS.'

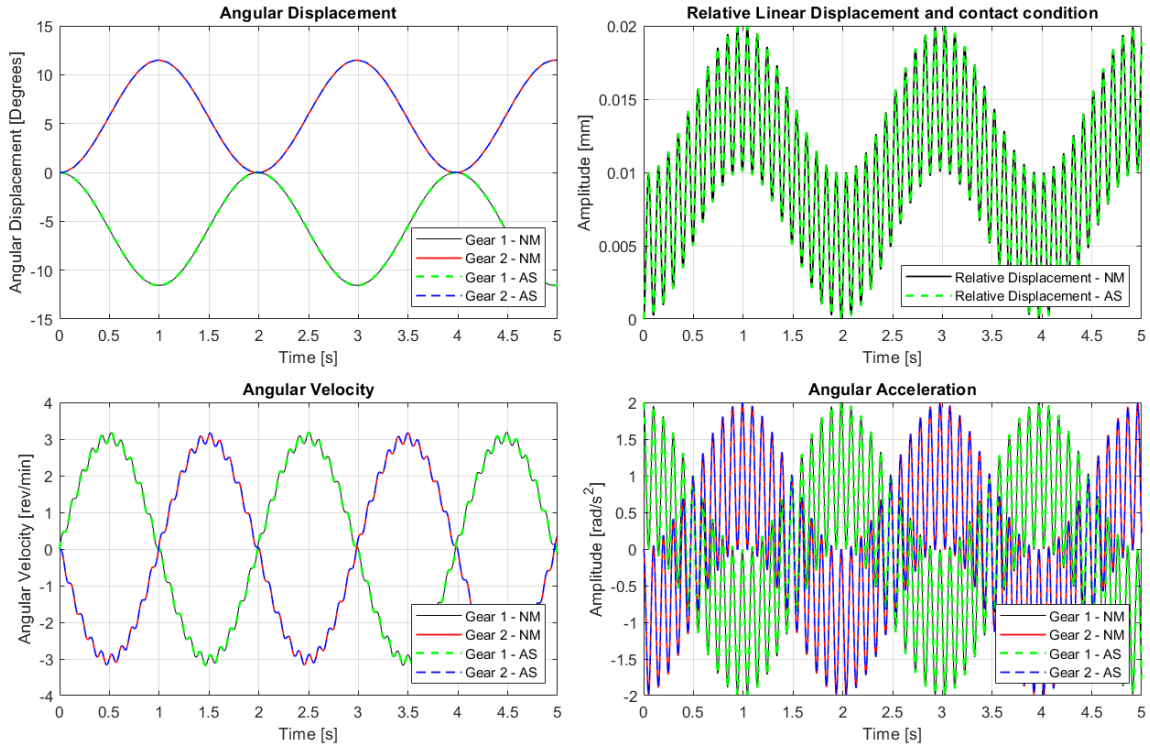

Figure 13. Comparison between Newmark and AMESim results using no backlash in the model, for the constant torque applied.

The AMESim and Newmark results shows consistent behavior for all parameters evaluated. The angular displacement

of gear 1 and gear 2 show the same results with inverted signs, as expected due to their opposing rotations. The relative linear displacement results show a small magnitude of displacement, even in the absence of backlash in the system. This phenomenon occurs due to the consideration of contact stiffness between the impact pair, leading to oscillations depending on stiffness values, even without backlash. This hypothesis was confirmed by observing that with the increase of the contact stiffness, the maximum relative linear displacement value were reduced.

For the model with $1mm$ backlash, show in Fig. 14, the contact condition indicates if there is contact between the gears at a given integration time. The contact condition is equal to -1 if the gears are in contact by the right side of the gears tooth, zero when no contact exists, and equal to 1 if they are in contact by the left side of the gear tooth.

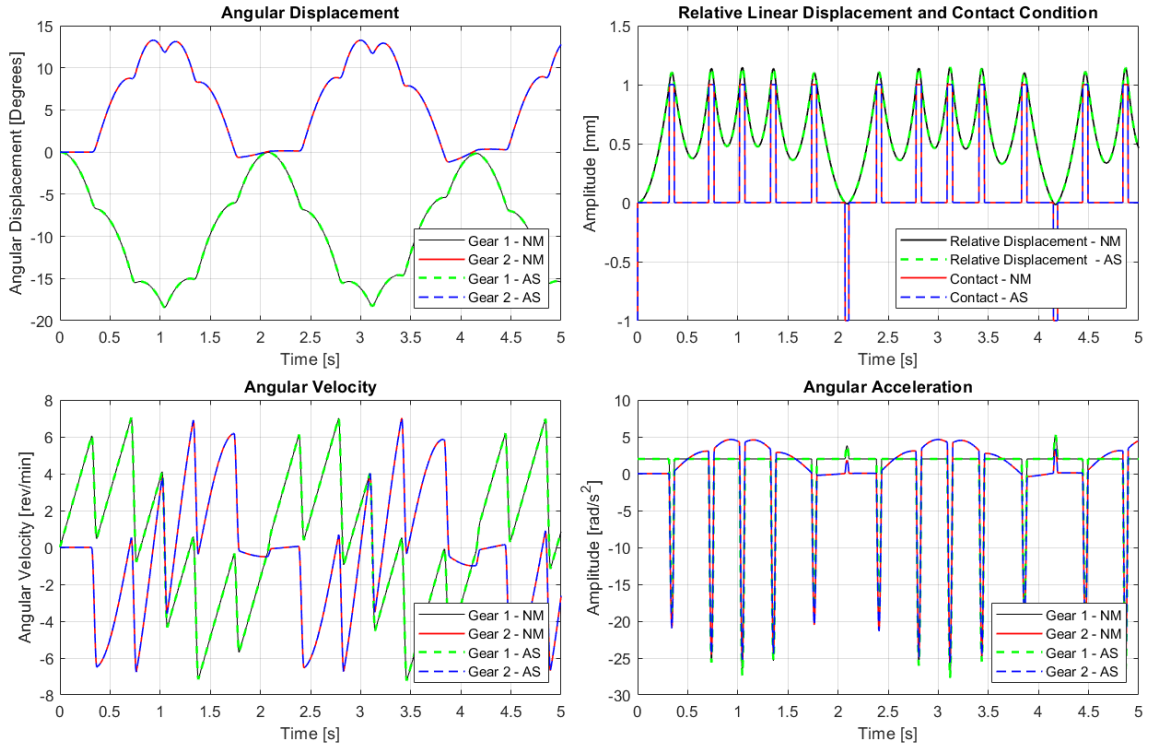

Figure 14. Comparison between Newmark and AMESim results using $1mm$ of backlash in the model, for the constant torque applied.

Both methods show great similarity between their results. The angular displacement of the second gear, displayed in red, doesn't show any displacement until 0.33s, which is expected and occurs given the inclusion of the backlash in the system. This was confirmed by the contact condition graph, which showed no contact until 0.33 seconds and then transitioned to 1, indicating right-side contact. After 0.33s, the angular displacement of the gear 2 increased, and gear 1's displacement slightly decreased, reflecting their contact.

In the results, around 2.07s and 4.14s, it indicates a slight contact by the left side of the gears tooth. The angular velocity and angular acceleration confirms that the slight contact, as in the velocity graph show a small change in the velocity behavior, most visible in the gear 2 result. In the acceleration graph also shows a small peak in acceleration of both gears around 2.07s and 4.14s, in inverse sign when compared with the other impacts observed before, which confirms that the impact occurred in a different direction than other impacts.

Differences between angular displacement and relative linear displacement between the gears were analyzed using the mean absolute error (MAE) and the mean percentage error (MPE). Table 2 presents the differences obtained between the AMESim and Newmark methods.

Table 2. Mean Absolute Error (MAE) and Mean Percentual Error (MPE) differences between AMESim-Newmark displacements and relative displacements.

Backlash (mm)	**Parameter**	**AMESim-Newmark (MAE)**	**AMESim-Newmark (MPE%)**
0	Displacement	1.25E-05	1.16E-02
	Relative Displacement	4.35E-06	1.73E-01
1	Displacement	4.17E-05	1.30E-03
	Relative Displacement	1.26E-05	8.00E-03

The results presented in Table 2 demonstrate a good displacement and relative displacement convergence in the evaluated cases. In the obtained mean percentage error values presented a slight higher value due to the results of displacement and relative displacement gets closer to zero, and in these cases the percentage values shows an increase in its value because of the reference value been close to zero.

To assess the system behavior, the phase diagrams of both configurations of backlashes used were generated. Figure 15 displays the phase diagram of the model with no backlash on the left, and the model with $1mm$ backlash on the right.

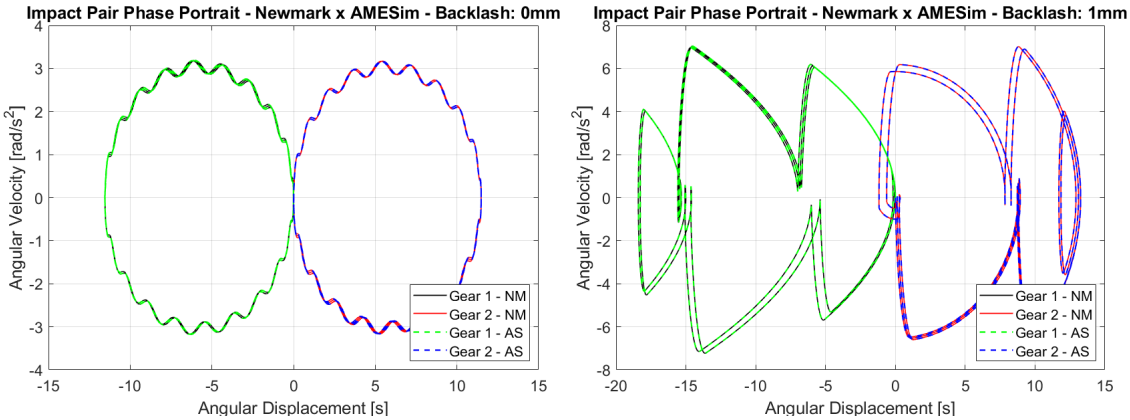

Figure 15. Phase diagrams of the model, without backlash on the left, with $1mm$ backlash on the right.

The phase diagram with no backlash shows a symmetric response in relation to the vertical axis between both gears of the model, as expected since both gears rotate with the same speed in inverse direction, given that the gear relation used in the model was a 1:1 ratio. The phase diagram considering a $1mm$ backlash presents higher variations in the velocity axis; it shows that initially the input gear rotates freely with no contact with the output gear.

The input gear rotates freely from the initial position, found where both angular displacement and angular velocity are equals to zero, until they reach the point where the angular displacement is equal to -5.7 and angular velocity equal to 6.0, after this point, the gears enter a contact regiment and the output gear start to rotate and gather velocity. For the input gear, the contact goes from where the angular displacement is equal to -5.7 and angular velocity equal to 6.0 until the angular displacement reach the value of -6.7 and angular velocity equals to 0.5. For the output gear, the contact goes from where angular displacement and angular velocity are equal to zero, until they reach the values of 1.0 for angular displacement and -6.4 for the angular velocity. After the contact regiment the gears rotate freely, the input gear starts to gather speed again and the output gear decreases its speed, until they enter in contact again where angular displacement is equal to -14.4 and angular velocity equal to 7.0 for the input gear, until angular displacement reaches 8.7 and angular velocity reaches 0.5 for the output gear.

5. CONCLUSION AND FUTURE WORK

This research reviewed important points necessary to implement the nonlinear Newmark method, also compared and validated the results of two different models with a commercial software to ensure precision and accuracy of the implementation. First, the nonlinear model showed good convergence with the commercial software considering the different values of α, and obtaining a range of mean percentual error between 4.20E-07 to 6.08E-04.

The comparison of the Newmark's impact pair results with the comercial software showed great similarity with both backlashes considered in the model. With no backlash the results were concise between AMESim and Newmark's method, even in the theoretical values of relative displacement between the gears found was identical in both methods. Since the backlash was considered zero in this case, theoretically the relative displacement results should also be found close to zero, but tests changing the contact stiffness between the gears showed that with the increase of the stiffness the relative displacement magnitude was decreased, indicating that these phenomena occurs due to the consideration of a stiffness between the impact pair, and not considering an ideal contact.

With the inclusion of the backlash, the Newmark method was able to detect even smaller impacts between the impact pair, as showed on the right side impact situations in Fig. 13, which indicates that the utilization of Newmark's method to analyze vibroimpacts would precisely characterize these phenomena with remarkable sensitivity.

This analysis examined the system's vibrational response and overall performance. By scrutinizing Newmark's results, valuable insights were gained into the system's behavior and its interaction between the gear pairs. To guarantee the credibility and reliability of the suggested approach, a comparative assessment was conducted by benchmarking Newmark's results against those obtained from AMESim, which verified great concordance between their results.

Through this evaluation process, the research provides a comprehensive understanding of the system's dynamics, mainly focusing on gear rattle and clunk noise phenomena. The knowledge gained from this study will contribute to

advancing design methodologies for transmission systems, enabling engineers to optimize gear designs and mitigate noise and vibration issues effectively.

6. ACKNOWLEDGEMENTS

This project is a collaborative partnership between UNICAMP and EATON Ltda. We want to express sincere gratitude to Eaton Ltda for funding this project.

7. REFERENCES

Chen, X. *et al.*, 2018. "Effects of macro-parameters on vibration and radiation noise for high speed wheel gear transmission in electric vehicles". *Journal of Mechanical Science and Technology*. doi:10.1007/s12206-018-0813-5.

Chopra, A.K., 1995. *Dynamics of Structures: Theory and Aplications to Earthquake Engineering*. Prentice Hall, Englewood Cliffs, New Jersey.

Comparin, R., 1988. *A Study of the Frequency Response of Impact Pairs with Application To Automotive Gear Rattle*. Ph.D. thesis, Department of Mechanical Engineering, Ohio State University.

Crowther, A.R., Zhang, N. and Singh, R., 2005. "Development of a clunk simulation model for a rear wheel drive vehicle with automatic transmission". In *SAE Technical Paper*.

Geradin, M. and Rixen, D.J., 2014. *Mechanical Vibrations: Theory and Application to Structural Dynamics, 3rd Edition*. John Wiley and Sons, Hoboken, New Jersey, EUA.

Gurm, J.S., Crowther, A.R., Singh, R. *et al.*, 2007. "Transient clunk response of a driveline system laboratory experiment and analytical studies". In *SAE Technical Paper*. 2007-01-2233.